Synthetic Metals 185–186 (2013) 115–119

Contents lists available at ScienceDirect

Synthetic Metals

journal homepage: www.elsevier.com/locate/synmet

Low-boiling-point solvent additives can also enable morphological control in polymer solar cells

Rakesh C. Mahadevapuram[a], John A. Carr[b], Yuqing Chen[b], Sayantan Bose[c], Kanwar S. Nalwa[b], Jacob W. Petrich[c], Sumit Chaudhary[a,b,*]

[a] Department of Materials Science and Engineering, Iowa State University, Ames, IA, USA
[b] Department of Electrical and Computer Engineering, Iowa State University, Ames, IA, USA
[c] Ames Laboratory and Department of Chemistry, Iowa State University, Ames, IA 50011, USA

ARTICLE INFO

Article history:
Received 5 July 2013
Accepted 6 October 2013

Keywords:
Organic solar cells
Solvent additives
Morphology

ABSTRACT

Processing organic photovoltaic (OPV) blend solutions with high-boiling-point solvent additives has recently been used for morphological control in bulk-heterojunction OPV cells. Here we show that even low-boiling-point solvents can be effective additives. When P3HT:PCBM OPV cells were processed with a low-boiling-point solvent tetrahydrafuran as an additive in parent solvent o-dichlorobenzene, charge extraction increased leading to fill factors as high as 69.5%, without low work-function cathodes, electrode buffer layers or thermal treatment. This was attributed to PCBM demixing from P3HT domains and better vertical phase separation, as indicated by photoluminescence lifetimes, hole mobilities, and shunt leakage currents. Dependence on solvent parameters and applicability beyond P3HT system was also investigated.

1. Introduction

Solution processed bulk-heterojunction (BHJ) OPV cells have found immense interest due to the promise of low-cost roll-to-roll fabrication on flexible substrates, among other reasons. In a BHJ cell, photogenerated electron–hole pairs (excitons) dissociate at the donor–acceptor interface, and electrons and holes are transported to respective electrodes. Efficient exciton dissociation requires donor–acceptor intermixing at the scale of exciton dissociation length (ca. 10 nm), and efficient transport requires larger domains enabling percolating pathways. Thus, optimizing BHJ morphology requires delicate balance between optimizing both of these processes.

Recently, power conversion efficiencies around 8% have been achieved in BHJ OPVs [1,2]. To obtain high efficiencies in P3HT:PCBM cells, techniques like thermal and solvent annealing are typically used [3,4]. However, for cells based on emerging push–pull polymers, thermal annealing typically degrades the performance [5], and utilizing high-boiling-point (high-bp) solvent additives has emerged as an alternative method to improve efficiencies. Such additives optimize BHJ morphology in one of the following ways: enhance polymer crystallinity and optical absorption [6]; create finer morphology for efficient exciton dissociation [7,8]; or increase inter-connected pathways for better charge transport [9]. These high-bp solvent additives are able to do so either by selective dissolution of one of the species like fullerenes [8,9], or by better dissolution of the entire polymer-fullerene blend [6,7], or by being a marginal solvent for both species [10].

Here we show a deviation from the conventional rule on solvent additives. We show that even a low-bp solvent additive (tetrahydrofuran (THF)) in a high-bp parent solvent (o-dicholorobenzene (ODCB)) is able to control nanomorphology in P3HT:PCBM cells, leading to efficient charge extraction and fill factors (*FF*) as high as 69.5% (67.5 ± 0.9%). These are among the highest *FF* recorded (~68%) [11] for the P3HT:PCBM system. It should be noted that we obtained such high *FF* without any thermal treatment, or low work-function cathodes like Ca, or charge blocking buffer layers like TiO*x*. *FF* of the control ODCB device was 64.2% (±2.1%). Overall efficiencies however were comparable for both, devices with THF additive (ODCB-THF devices) and ODCB-only devices, due to slight reduction in short-circuit-current (J_{sc}) for ODCB-THF device (reasons discussed in Section 2). However, the significance of this study lies in: (1) improving the charge extraction (*FF*), which is typically more challenging than increasing J_{sc}; J_{sc} can be more easily enhanced by increasing film thickness or utilizing an optical spacers; (2) demonstrating that even though low-bp additive evaporates before the parent solvent, morphological changes induced by it persist in the solid-state film. A recent report has also mentioned the use of a solvent additive dimethyl formamide with boiling-point

* Corresponding author at: 2124 Coover Hall, Iowa State University, Ames, IA 50011, USA. Tel.: +1 515 294 0606.
E-mail address: sumitc@iastate.edu (S. Chaudhary).

0379-6779/$ – see front matter © 2013 Elsevier B.V. All rights reserved.
http://dx.doi.org/10.1016/j.synthmet.2013.10.004

(153 °C) only slightly lower than the parent solvent ODCB (180 °C) to improve the performance of PCDTBT:$PC_{71}BM$ based OPVs [1]. However, in our study, the bp of the additive THF is significantly lower (66 °C). For comparison purposes, we also fabricated devices with commonly used high-bp solvent additives octanedithiol (OT) and N-methyl 2-pyrollidine (NMP) in the parent solvent ODCB. For our low-boiling-point solvent additive approach, we also shed light upon dependence (or lack of) on slight variations in bp and solvent dipole moment, and applicability beyond the P3HT:PCBM system.

2. Materials and methods

The P3HT:PCBM based solar cells were fabricated on indium tin oxide (ITO) coated glass substrates (15 Ω/sq; Delta technologies). ITO coated substrates were cleaned by ultrasonication in acetone, isopropanol, detergent and water, and then subjected to air plasma cleaning for 5 min. PEDOT:PSS (Baytron4083 PVP) solution was spin-coated at 4000 rpm for 60 s on the clean ITO slides, followed by baking at 120 °C for 10 min, and transfer to Argon-filled glove box. 11 mg/ml (1:1) P3HT:PCBM mixture was dissolved in ODCB and stirred for ca. 18 h at 45 °C. The solution was then filtered using a 0.2 μm filter. The low-bp solvent additive THF with bp of 66 °C preferentially dissolves P3HT over PCBM. The high-bp solvent additives chosen were NMP (bp = 210 °C) and OT (bp = 270 °C), and both show greater affinity for PCBM dissolution. The host solvent ODCB has a bp of 186 °C and it is a good solvent for both P3HT and PCBM. Four solutions with 10 mg/ml final solute concentration were prepared by adding 10% by volume of THF, NMP, OT and ODCB to 90% by volume of ODCB based 11 mg/ml solutions of P3HT:PCBM. The solutions were stirred at 45 °C for 1 h and then spin-coated onto the PEDOT:PSS coated ITO substrates at 600 rpm for 40 s. All the spin-coated films were allowed to dry inside the same Petri-dish and their drying times were noted. The ODCB only and ODCB-THF films took 15–20 min to dry completely and the ODCB-OT and ODCB-NMP films took 25–30 min. The drying times noted were on the basis of visual inspection of change in color from orange to purplish pink. The dried films were then deposited with 150 nm of Al (top electrode) at 0.5 nm/s rate under pressure of 1×10^{-6} mbar in a thermal evaporator. No pre-production or post-production thermal annealing was performed on these films. Photocurrent density versus voltage characteristics were measured by illuminating the devices using an ELH quartzline lamp operating at 1 sun conditions, i.e. 100 mW/cm^2, calibrated using a standard crystalline silicon photodiode reference with a KG-5 filter. To obtain the thickness of films, a scratch was made on the film and the Atomic Force Microscope tip was scanned across the height profile in tapping mode. EQE measurements were done using ELH quartzline halogen lamp and a monochromator with a lock-in amplifier to eliminate background noise. The reference was a calibrated Si photodiode with known EQE spectra.

For the fabrication of PCDTBT:$PC_{71}BM$ based cells, the device structure was (PEDOT:PSS)/PCDTBT:$PC_{71}BM$/Ca/Al. Active layer was deposited from a solution containing PCDTBT:$PC_{71}BM$ (1:3.5) (from 1-Material) with a total concentration of 7 mg/ml in ODCB. Prior to spin-coating, this solution was stirred on a hot-plate at 90 °C or 8 h and subsequently at 60 °C for a few days. Two low-boiling-point organic solvents THF (bp = 66 °C) and chloroform (bp = 61 °C) were incorporated as additives in the original blend solution in a 10% (v/v) ratio. Electrode deposition and device characterization was done as mentioned for P3HT based devices.

3. Results and discussion

Three types P3HT:PCBM cells were fabricated with THF, OT and NMP as solvent additives (10% volume) in parent solvent ODCB

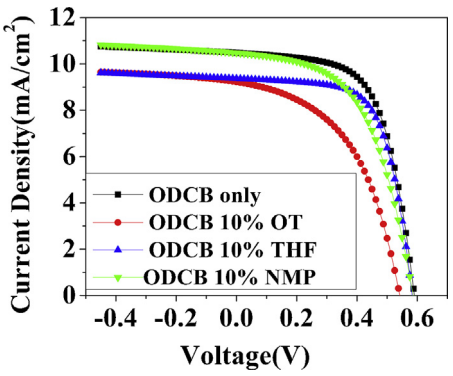

Fig. 1. Typical current vs. voltage characteristics (under AM 1.5G illumination) of the four types of P3HT:PCBM devices studied.

(90% volume). Control device utilized only ODCB as the solvent (see Supporting Information for fabrication details). The low-bp solvent additive THF (bp = 66 °C) preferentially dissolves P3HT; high-bp solvent additives NMP (bp = 210 °C) and OT (bp = 270 °C) preferentially dissolve PCBM; and the host solvent ODCB (bp = 186 °C) is a good solvent for both P3HT and PCBM. The active-layer thicknesses for ODCB, ODCB-THF, ODCB-OT, and ODCB-NMP devices were ca. 150 nm, 135 nm, 110 nm, and 170 nm, respectively. Thicknesses were different despite identical processing conditions due to differential wetting of solvent mixtures on PEDOT:PSS coated ITO substrates.

Photocurrent density versus voltage plots are shown in Fig. 1 for the four types of devices with ODCB-THF device exhibiting *FF* of 68%, which was 8% higher than *FF* of the ODCB device. These plots are only for one set of devices representative of their relative performance. Overall, we fabricated 24 cells of each device type in four different batches over a period of several weeks. Table 1 summarizes the statistical device characteristics of all devices. As can be seen, ODCB-THF device always showed the highest *FF*, and was the most reproducible device (least standard deviation). Overall performances of ODCB devices and ODCB-THF devices were comparable due to slightly reduced J_{sc} in ODCB-THF devices. This can be partly ascribed to lower photon harvesting in ODCB-THF devices as the active-layer thickness was less than the ODCB devices. It should be noted though that less active-layer thickness of ODCB-THF film was not the reason behind higher *FF*, as we have fabricated several ODCB only devices of lesser thicknesses in our laboratory, and never achieved 68% *FF*. Morever, the thinnest active-layer (ODCB-OT case) led to worst *FF*. Thus the origin of high *FF* must be due to a morphological change caused by THF, which we characterized further as discussed below.

External quantum efficiency (EQE) of devices followed the same trend as J_{sc}, as expected. However, normalized QE curves (Fig. 2a) show that ODCB-THF device had the highest relative photocurrent at higher wavelengths, indicating highest effective conjugation length of P3HT. Further, ODCB-THF films had the highest photoluminescence (PL) lifetime (Fig. 2b), which also indicates toward largest P3HT domains in ODCB-THF films. Large domain sizes lead to low singlet-exciton dissociation efficiency, and thus high PL lifetime. Thus, both QE and PL lifetimes unambiguously show that P3HT domain sizes are largest in ODCB-THF devices, and that is in some way leading to best charge extraction and highest *FF* in ODCB-THF devices. Considering the relative solubilities of P3HT and PCBM in THF, one can understand why P3HT domains were largest in ODCB-THF films. Recently, neutron scattering characterization of P3HT:PCBM films showed that such films have the '*rivers and streams*' [12] morphology with three types of domains: crystalline P3HT, amorphous mixture of P3HT and PCBM, and crystalline PCBM [12]. Thus, since PCBM is insoluble in THF, demixing of PCBM from

Table 1
Performance parameters of the four types of P3HT:PCBM devices studied (24 contacts of each type spread across 4 batches).

Sample	V_{oc}	J_{sc}	*FF*	PCE
ODCB	0.59 ± 0.01	10 ± 0.7	64.2 ± 2.1	3.79
ODCB-THF	0.58 ± 0.00	9.5 ± 0.4	67.5 ± 0.9	3.74
ODCB-OT	0.53 ± 0.02	9.1 ± 0.4	45.1 ± 4.3	2.17
ODCB-NMP	0.58 ± 0.01	10.4 ± 0.8	56.9 ± 1.5	3.41

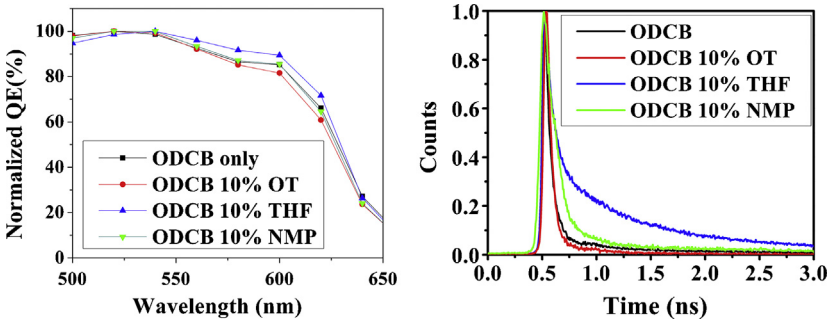

Fig. 2. (left) Normalized QE, and (right) PL lifetimes of active-layers for the four types of P3HT:PCBM devices. Normalized QE was obtained by setting the maxima of EQE curves at 100%.

amorphous mixture of P3HT and PCBM is promoted. This leads to decreased number of donor–acceptor interfaces for exciton dissociation reflected in PL lifetimes. However, charge extraction and *FF* improves as a result of this demixing.

To elucidate the origin of better charge extraction, we measured electric field dependent space-charge-limited-current hole mobilities in hole only P3HT:PCBM diodes using MoO_3/Al as the top electrode. Zero-field hole mobilities obtained for ODCB, ODCB-THF, ODCB-OCT and ODCB-NMP were 1.54×10^{-3} cm^2/Vs, 1.39×10^{-3} cm^2/Vs, 4.61×10^{-3} cm^2/Vs and 7.05×10^{-3} cm^2/Vs, respectively. The hole mobilities in ODCB and ODCB-THF devices were better than ODCB-OT and ODCB-NMP devices. However, the mobilities were similar for ODCB and ODCB-THF devices. This shows that demixing of PCBM from P3HT:PCBM domains does not result in increased hole mobility in P3HT, and thus better hole transport is not the reason behind enhanced *FF* in ODCB-THF devices. We also estimated trap densities using capacitance measurements [13] and trap densities were in the order of 10^{16} cm^{-3} for all four devices.

To probe the charge extraction aspect, we also evaluated dark current versus voltage characteristics. The shunt leakage current, that is, the current at low forward bias was higher for ODCB device than ODCB-THF device (Fig. 3). Traditionally, shunt leakage current has been attributed to a parallel resistance in the circuit model. However, recently it was shown that for all thin film photovoltaics including OPVs, shunt leakage current is non-ohmic in nature and follows a space-charge-limited-current type model [14], in which,

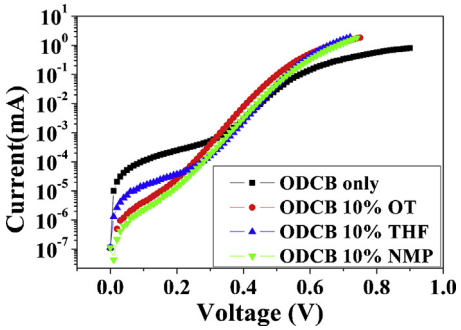

Fig. 3. Dark current vs. voltage characteristics for the four types of P3HT:PCBM devices.

higher charge mobilities lead to higher shunt leakage currents. This partly explains why shunt leakage currents for ODCB-OT and ODCB-NMP devices were the lowest. But despite having similar values of hole mobilities, the shunt leakage current for ODCB device is higher than ODCB-THF device. This indicates toward a higher number of shunt paths in the ODCB device, or in other words, poorer vertical phase segregation in which more P3HT and/or PCBM paths percolate from one electrode to another. Thus, we can deduce that although THF leads to demixing of PCBM from the amorphous P3HT:PCBM regions, it does not increase the overall crystallinity (and hole mobility) of P3HT. It does however promote a better vertical phase segregation, thus less shunt leakage, and as a result higher charge extraction and *FF*. We also performed AFM imaging on our films. RMS surface roughnesses were found to be similar – 9 nm, 5.6 nm, 5.9 nm and 6.2 nm for ODCB, ODCB-THF, ODCB-OT and ODCB-NMP, respectively. However, phase images (Fig. 4) show that the surface of ODCB-NMP and ODCB-OT films have striations that are ascribed to the presence of P3HT lamellas [15]. Such P3HT lamellas will inhibit electron collection at the cathode, which further explains poor *FF* for ODCB-OT and ODCB-NMP devices.

The aforementioned behavior of ODCB-THF films led us to the question: how does device performance depend on or vary with change in solubility parameters of THF? To characterize this, we also investigated other solvents in THF family as additives. To test dependence on boiling point, we utilized THF (bp = 66 °C), dimethyl THF (bp = 92 °C), and diethyl THF (bp = 155 °C) as the solvent additives in ODCB parent solvent. Fig. 5 shows that device performance was insensitive to variation in bp and all three devices performed quite similarly. To test dependence on the polarity of the solvent, we utilized THF (dipole moment = 1.65 D), methyl furan (0.63 D), and acetonitrile (3.92 D) as solvent additives in ODCB parent solvent. Fig. 5 shows that device performance slightly improves with increase in dipole moment of the additive, although THF and acetonitrile devices behaved quite similarly. This correlation with dipole moment was not reproducible, which indicates that the dependence between performance and dipole moments is weak. Thus, we conclude that the morphological effect of THF additive is more of a function of its preferential affinity for P3HT over PCBM, than its bp; this preferetial affinity is also only weakly affected by change in the dipole moment of the solvents in THF family.

Finally, we were curious about the generality of the low-boiling-point solvent approach across other OPVs based on other material

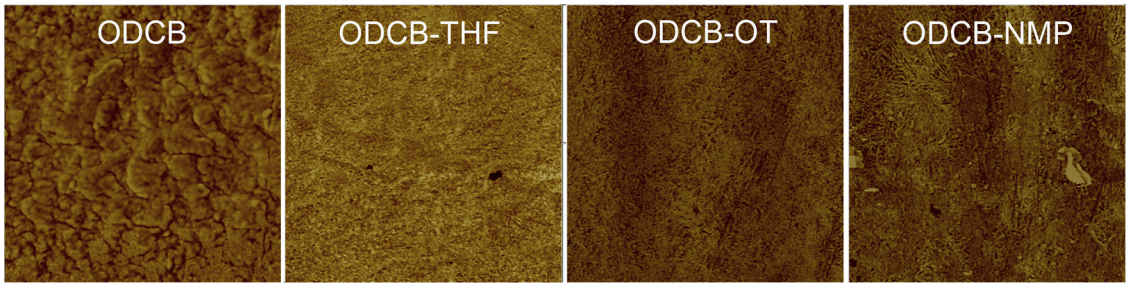

Fig. 4. Atomic force microscope phase images of the four types of P3HT:PCBM films.

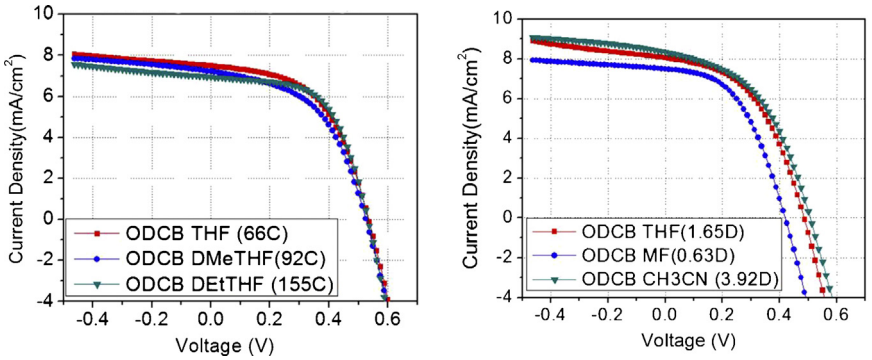

Fig. 5. Typical current vs. voltage characteristics (under AM 1.5G illumination) of the devices with THF derivatives as solvent additives: (left) THF, dimethyl THF (DMeTHF), and diethyl THF (DEtTHF) derivatives with varying boiling points, and (right) THF, methyl furan (MF), and acetonitrile (CH3CN) derivatives with varying dipole moments.

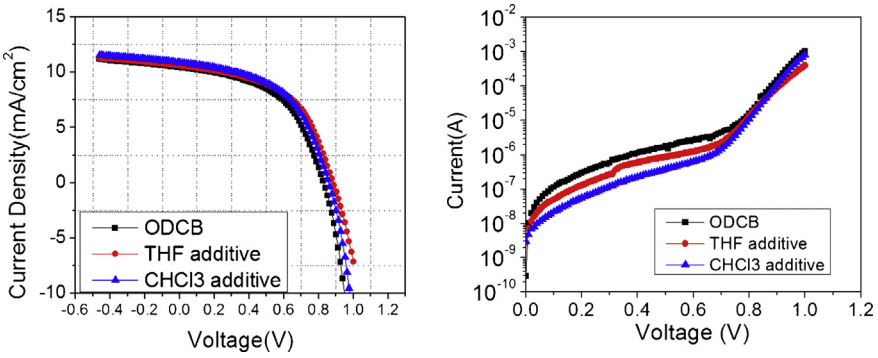

Fig. 6. Current vs. voltage characteristics of PCDTBT:PC_{71}BM devices under illumination (left) and in dark (right).

systems. As an exemplary case, we investigated PCDTBT:PC_{71}BM based OPV devices. In addition to control PCDTBT:PC_{71}BM devices fabricated from parent solvent ODCB, we also fabricated devices with THF and $CHCl_3$ additives (10% by volume in parent solvent ODCB. See Section 2 for experimental details.). Current–voltage curves of these devices are shown in Fig. 6, and performance parameters are listed in Table 2. Both ODCB-THF and ODCB-$CHCl_3$ devices show a slight improvement over the control in all the three aspects – V_{oc}, J_{sc}, and *FF*. Similar to the case of P3HT:PCBM devices, devices with both low-boiling-point additives showed reduced shunt leakage currents. Thus, we expect that in the case of PCDTBT:PC_{71}BM devices also, the additives slightly improve the overall vertical phase separation (appropriate donor–acceptor connectivity between the electrodes), which leads to higher V_{oc} and *FF*. Unlike the case of P3HT:PCBM, J_{sc} does not suffer (in fact it slightly increases) for additive based PCDTBT devices. This is probably because of much higher fullerene loading in these devices, which can be expected to alleviate the negative consequence of polymer-fullerene demixing. Observed difference in the performance of our three device-types is not large, but it is not the upper bound as the additive concentration is not optimized. However, similar to the P3HT:PCBM case, these devices again demonstrate that even though a low-boiling-point additive evaporates much before the parent solvent, the morphological changes induced by it persist in the dry film.

Table 2
Performance parameters of the three types of PCDTBT:PC_{71}BM devices.

Sample	V_{oc}	J_{sc}	*FF*	PCE
ODCB	0.83	10.44	52.1	4.51
ODCB-THF	0.88	10.59	52.6	4.92
ODCB-$CHCl_3$	0.86	10.87	52.4	4.89

4. Conclusions

Conventional rule on utilization of solvent additives in BHJ OPV cells is that additives should have a higher bp (lower vapor pressure) than the parent solvent, so that additives can stay longer in the film and affect morphology. Main conclusion of our study is

that this is not necessarily true. We showed that even though a lower bp additive evaporates faster than the parent solvent at large, at least traces of it evidently stay in the drying film for longer, and lead to morphological changes that persist in the solid-state film. This was demonstrated for P3HT:PCBM and PCDTBT:C_{71}BM material systems.

Acknowledgements

This work was primarily (experimental design, device fabrication and characterization) supported by National Science Foundation (ECCS-1055930). PL lifetime studies were supported by the U.S. Department of Energy, Office of Basic Energy Sciences, through the Ames Laboratory. The Ames Laboratory is operated for the U.S. Department of Energy by Iowa State University under Contract No. DE-AC02-07CH11358.

References

[1] T.Y. Chu, et al., Appl. Phys. Lett. 98 (2011) 253301.
[2] Y. Liang, Z. Xu, J. Xia, S.T. Tsai, Y. Wu, G. Li, C. Ray, L. Yu, Adv. Mater. 22 (2010) E135.
[3] F. Padinger, R.S. Rittberger, N.S. Sariciftci, Adv. Funct. Mater. 13 (2003) 85.
[4] G. Li, Y. Yao, H. Yang, V. Shrotriya, G. Yang, Y. Yang, Adv. Funct. Mater. 17 (2007) 1636.
[5] Z.M. Beiley, E.T. Hoke, R. Noriega, J. Dacua, G.F. Burkhard, J.A. Bartelt, A. Salleo, M.F. Toney, M.D. McGehee, Adv. Energy Mater. 1 (5) (2011) 954.
[6] F.C. Chen, H.C. Tseng, C.J. Ko, Appl. Phys. Lett. 92 (2008) 103316.
[7] C.V. Hoven, X.D. Dang, R.C. Coffin, J. Peet, T.Q. Nguyen, G.C. Bazan, Adv. Mater. 22 (2010) E63.
[8] S.J. Lou, J.M. Szarko, T. Xu, L. Yu, T.J. Marks, L.X. Chen, J. Am. Chem. Soc. 133 (2011) 20661.
[9] J.K. Lee, W.L. Ma, C.J. Brabec, J. Yuen, J.S. Moon, J.Y. Kim, K. Lee, G.C. Bazan, A.J. Heeger, J. Am. Chem. Soc. 130 (2008) 3619.
[10] L. Chang, H.W.A. Lademann, J.B. Bonekamp, K. Meerholz, A.J. Moule, Adv. Funct. Mater. 21 (2011) 1779.
[11] G. Dennler, M.C. Scharber, C.J. Brabec, Adv. Mater. 21 (2009) 1323.
[12] W. Yin, M. Dadmun, ACS Nano 5 (2011) 4756.
[13] P.P. Boix, G. Garcia-Belmonte, U. Muecas, M. Neophytou, C. Waldauf, R. Pacios, Appl. Phys. Lett. 95 (2009) 233302.
[14] S. Dongaonkar, J.D. Servaites, G.M. Ford, S. Loser, J. Moore, R.M. Gelfand, H. Mohseni, H.W. Hillhouse, R. Agrawal, M.A. Ratner, T.J. Marks, M.S. Lundstrom, M.A. Alam, J. Appl. Phys. 108 (2010) 124509.
[15] B. Tremolet de Villers, C.J. Tassone, S.H. Tolbert, B.J. Schwartz, J. Phys. Chem. C 113 (2009) 18978.